Research Square

Preprints are preliminary reports that have not undergone peer review.
They should not be considered conclusive, used to inform clinical practice,
or referenced by the media as validated information.

Assess land use changes and the impact on population change across the Hong Kong-Zhuhai-Macao Greater Bay Area Urban Clusters

Xiaotong Su
Macao Polytechnic University
Patrick Pang
mail@patrickpang.net

Macao Polytechnic University
Ting Liu
Macao Polytechnic University
Yiming Taclis Luo
Macao Polytechnic University
Kin SunChan
University of Macau

Article

Keywords: Hong Kong-Zhuhai-Macao Greater Bay Area, Urban Clusters, Land use, Population dynamics, Hot spot analysis

Posted Date: November 16th, 2026

DOI: https://doi.org/10.21203/rs.3.rs-11523017/v1

License: This work is licensed under a Creative Commons Attribution 4.0 International License.
Read Full License

Additional Declarations: No competing interests reported.

Assess land use changes and the impact on population change across the Hong Kong-Zhuhai-Macao Greater Bay Area Urban Clusters

Xiaotong Su[a.], Patrick Pang[a.]*,Ting Liu[a.], Yiming Taclis Luo[a.] and Kin SunChan[b.]

[a.] Faculty of Applied Sciences, Macao Polytechnic University, Macao 999078, China;

[b.] Department of Government and Public Administration, Faculty of Social Sciences, University of Macao

p2523603@mpu.edu.mo(X.S.);p2314982@mpu.edu.mo(T.L.);p2417889@mpu.edu.mo(Y.T.L.) and kschan@um.edu.mo(K.S.C)

*Correspondence: mail@patrickpang.net

Abstract

Hong Kong, Zhuhai, and Macao Greater Bay Area Urban Clusters (HZM-GBAUC) collectively constitute one of the world's most densely populated and institutionally diverse cross-boundary metropolitan clusters. This study systematically evaluates land use conditions across the HZM-GBAUC at four discrete time points spanning 2016 to 2025, integrating four corresponding periods of population density data. Employing a land use transfer matrix, a spatial center-of-gravity migration model, and the Getis-Ord Gi* hot spot analysis, this study conducts a quantitative analysis of multi-source remote sensing land use data and demographic statistics through the ArcGIS 10.7 platform. The findings indicate that Zhuhai displays high-intensity population agglomeration across its entire territory; Hong Kong's population distribution is redistributing outward from the urban core toward the peripheral New Territories; and Macao's Cotai reclamation area has facilitated directed population transfer into newly developed built zones. The hot-cold patterns of population growth align broadly with the spatial trajectories of built-up land expansion across the HZM-GBAUC. For the first time, under a unified conceptual framework, the spatio-temporal mechanisms governing land–population linkages across Hong Kong, Zhuhai, and Macao are examined, offering suggestions for the global governance of high-density cross-boundary urban agglomerations in integrating diversified residential land supply.

Keywords: Hong Kong-Zhuhai-Macao Greater Bay Area; Urban Clusters; Land use; Population dynamics; Hot spot analysis

1. Introduction

In recent years, global research on land use change has shifted from quantitative expansion towards examining spatial quality [1]. Under the dual pressures of the global energy transition and food security, competition for land resources and land scarcity crises have intensified. The latest research focus on the interplay between emissions reduction targets, population carrying capacity, and food security [1].

Traditional models of population–land interaction have largely emphasised the linear relationship in which population growth drives the expansion of urban construction land [3]. However, recent empirical studies demonstrate that in highly urbanised or intensively developed areas, contemporary land use transitions are increasingly shaped by policy interventions [4], such as regional spatial planning, ecological red-line demarcations, and green economy legislation, rather than by demographic demand alone. Simultaneously, the negative feedback effects of land use change-induced environmental degradation on population dynamics are receiving growing attention [5]. Cross-disciplinary research integrating high-resolution remote sensing data with multi-dimensional environmental indicators, including land surface temperature and vegetation indices, has confirmed that localised urban heat islands and air pollutant concentrations resulting from built-up land expansion impose spatial environmental stress on elderly communities and vulnerable populations within affected areas [6]. Such deterioration in environmental quality is triggering intra-urban population mobility and spatial redistribution, rendering land use change an important variable in reshaping the patterns of population distribution [7].

Land use is widely employed in environmental research to reflect the natural attributes of land, referring to the long-term or cyclical productive activities that human societies undertake on land resources, guided by their natural characteristics and in pursuit of defined objectives, using biological and technical means. Land use change, in turn, denotes the evolutionary process by which land cover types, landscape patterns, and utilisation intensities are transformed across defined spatial and temporal scales, driven by both natural factors and human intervention [8]. This study employs the land use transfer matrix, a core analytical tool derived from the Markov model in systems analysis that characterises the direction and structural attributes of land use change [9], in conjunction with the temporal sequence of mutual conversions between different land use types at the beginning and end of the study period, to explain how land use not only quantitatively captures the overall trend in the area of each land category but also precisely delineates the internal logic of conversions between categories [10].

The completion of the Hong Kong-Zhuhai-Macao Bridge has triggered a cascade of changes in land use configuration and population mobility across the HZM-GBAUC [11]. While the empirical focus of this study is situated in the HZM-GBAUC, this region serves as far more than a local case study; it represents a quintessential testbed for addressing global urban and environmental challenges. Unlike conventional urban clusters, The HZM-GBAUC has become globally the most institutionally diverse and geographically interconnected cross-boundary cluster. It boasts extremely high population and building density, along with diverse institutional, economic, and urban planning standards. The unique typology of the HZM-GBAUC becomes particularly evident when compared to other world-class bay areas. For instance, the San Francisco Bay Area is primarily characterized by tech-driven innovation distributed across a relatively low-density, sprawling spatial structure under a unified national system. Conversely, the Tokyo Bay Area represents a mature, highly

industrialized, and high-density agglomeration, yet it benefits from the coordinated governance and standardized data frameworks of a single jurisdiction.

Land use change exerts a degree of influence on population change, defined as the dynamic evolution of population scale, spatial distribution, composition, and growth trends over time within a given area [12], in the context of this study, population change encompasses both quantitative shifts and spatial migration. An in-depth examination of the impacts of land use policy on population change over the past decade reveals that the relationship between population dynamics and land use is no longer simply one of land supply meeting demographic demand. For these developed and land-constrained cities, the influence of land use change has transcended mere physical necessity to become a pivotal factor in regulating the regional talent structure [13], balancing social welfare distribution, and alleviating social class tensions.

The Hong Kong, Zhuhai and Macao government have proposed leveraging the most efficient land-saving institutional arrangements to promote coordinated regional development and to facilitate the orderly mobility and optimised allocation of population across the HZM-GBAUC area [14][15]. Hong Kong's population management has undergone a transition over the past decade from monitoring-oriented approaches to active intervention [16]. The Hong Kong SAR Government has introduced a series of talent attraction measures to address the dual pressures of population outflow and accelerating ageing [17]. Data released by the Census and Statistics Department indicate that there remains a substantial inflow of people from mainland China and from across the globe. Macao's demographic structure has long been constrained by the dual limitations of extreme land scarcity and heavy dependence on the gaming and tourism industry [18]. Compared to Hong Kong, Macao's talent attraction schemes are more industry-oriented, targeting four key sectors: health and wellness, modern finance, high technology, and convention, trade, culture, and sports [19]. Zhuhai is positioned as a major nodal city within the Guangdong-Hong Kong-Macao Greater Bay Area, leveraging its land resources at scale to accommodate the spatial overflow of industry transferred from Macao and the living and service functions of residents [20]**Error! Reference source not found.**. With the continued improvement of port infrastructure, Zhuhai is undergoing a functional transformation from a traditional industrial city towards a life-services hub, accompanied by deep-seated adjustments in the residential structure of its permanent population and in its modes of land utilisation.

Land utilisation in the HZM-GBAUC is approaching saturation, and the elevated land premium has substantially raised the cost of living. For these developed and land-constrained cities, land use planning has transcended mere physical necessity to become a critical factor in regulating the regional talent composition, balancing social welfare distribution, and alleviating worker class tensions [22]. Hong Kong faces the dual pressures of population outflow and demographic ageing, relying heavily on external talent attraction without resolving the structural problem of endogenous population growth [23]. Constrained by extreme land scarcity, Macao is pursuing an industry-oriented talent attraction policy and urgently needs to expand its spatial capacity. Zhuhai, as a major node of the Greater Bay Area, is exploring cross-administrative-boundary land supply sharing models through platforms such as the Hengqin Guangdong-Macao In-Depth Cooperation Zone, accommodating the spillover of industries and residential functions from Macao [23].

Most existing research on land use change focuses on the developmental trajectories of individual cities. Few studies have delved deeply into the spatio-temporal linkages between land use change and population dynamics across adjacent cross-boundary urban agglomerations, and the

relevant research is in its early stages and remains incomplete. Moreover, no prior study has systematically revealed the spatio-temporal mechanisms governing land population linkages across Hong Kong, Zhuhai, and Macao within a unified conceptual framework. The objectives of this study are therefore as follows:

1. To provide a scientific basis for establishing cross-administrative-boundary land supply mechanisms, contributing to the integrated coordination of stock renewal in Hong Kong and Macao with incremental development in Zhuhai, and to avoid regional resource misallocation resulting from fragmented governance [24].

2. To guide governments in formulating land policies that diversify residential land supply and promote a balanced job–housing spatial structure, thereby enhancing the region's long-term capacity to attract high-caliber labor [25].

3. To reveal the land-population interrelationships that serve not only the high-quality development of Hong Kong, Zhuhai, and Macao, but also offer experience for the efficient management of land and the balanced distribution of population in high-density cross-boundary urban agglomerations globally [26].

Two core questions structure this research:

RQ 1: Are population changes across the HZM-GBAUC related to land use change? How do the direction and scale of built-up land expansion influence population dynamics in each city?

RQ 2: The spatio-temporal evolution of built-up land across the HZM-GBAUC exhibits phased characteristics, what is the relationship between the spatial trajectory of center-of-gravity migration and changes in regional population density?

2. Method

2.1 Overview of the study area

2.1.1 Geographical Overview

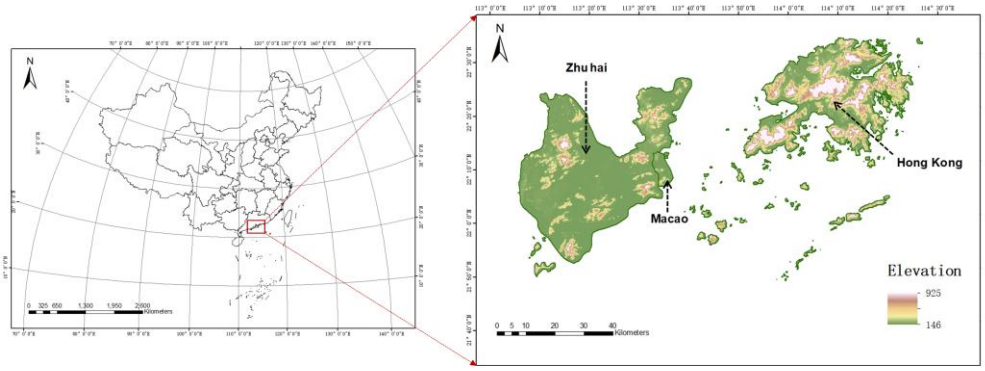


Figure 1 Geographical Overview of Hong Kong, Zhuhai, and Macao

As illustrated in Figure 1， Hong Kong, Zhuhai, and Macao are all situated along the southeastern coast of China, occupying the core zone of the Guangdong-Hong Kong-Macao Greater Bay Area and sharing a distinctive and closely interconnected spatial locational advantage. Hong Kong has a total land area of approximately 1,114 km²; its terrain is dominated by low hills, with

limited flat land. These constrained natural conditions have led to the formation of a high-density [27], vertically structured urban spatial pattern. Zhuhai and Macao share a direct land boundary. Zhuhai has a total land area of approximately 1,736 km² [28]; its coastline is intricate and its island groups are numerous, with landforms primarily comprising plains and low hills, offering a comparatively expansive land development hinterland **Error! Reference source not found.**. The Macao is situated in the southeastern part of Zhuhai, composed of the Macao Peninsula, Taipa Island, and Coloane Island [30]. Constrained by its historical development and extreme land scarcity, Macao has long relied on land reclamation projects to extend its urban boundaries; its land area has expanded from under 15 km² in the late nineteenth century to approximately 33.3 km² at present, making it one of the most representative cases of land use change in the region. Since the opening of the Hong Kong–Zhuhai–Macao Bridge, the HZM-GBAUC have achieved cross-sea direct connection, breaking down their physical barriers and providing a geographical basis for optimising the spatial structure of land use and enhancing connectivity within the urban agglomeration [32].

2.1.2 Population profile

The HZM-GBAUC exhibit significant differences in population size, density, and growth dynamics, closely linked to their respective land carrying capacities and urban functional orientations [32]. As a highly developed international metropolis, Hong Kong's current permanent resident population stands at approximately 7.5 million. The urban cores of Kowloon City District in particular maintain extremely high population densities. Macao is among the most densely populated territories in the world [33]; as of early 2024, its total population is approximately 686,000, with large numbers of people concentrated in the geographically small peninsula area. Zhuhai has maintained robust population growth in recent years; by 2024, its permanent resident population has surpassed 2.5 million, with an urbanisation rate exceeding 90% [34].

2.2 Dataset source

The primary data in this study are divided into land use data and population data.

Land use data were collected for the years 2016, 2019, 2022, and 2025. The 2016, 2019, and 2022 land use datasets are drawn from GLC_FCS30D: a global 30-m land-cover dynamic monitoring product with a fine classification system covering 1985 to 2022. GLC_FCS30D is the first global fine land cover dynamic product at 30-metre resolution to adopt continuous change detection. It employs a refined classification system containing 35 land categories spanning 1985 to 2022; update cycles were every five years prior to 2000 and annual thereafter. The 2025 land use data were sourced from the National Geomatics Centre of China [35][36][37].

Population data consist of population density datasets for Hong Kong, Zhuhai, and Macao for 2016, 2019, 2023, and 2024. These were obtained from the LandScan high-resolution global population distribution dataset, developed by the U.S. Department of Energy's Oak Ridge National Laboratory. As annual data are typically compiled in the following year, the 2024 population density data represent the most recent available observation [38].

2.3 Software and tools

Spatial data processing, cartographic visualisation, and core spatial statistical analyses in this study were conducted primarily using ESRI's ArcMap software platform (version ArcGIS 10.7) [39]. As a classical desktop GIS application, ArcMap offers powerful capabilities in spatial data management, topological editing, overlay analysis, and spatial modelling, enabling efficient processing of multi-source heterogeneous data [40], including raster data extracted from post-classification remote sensing imagery and vector-format census data. Specifically, the data

management tools in ArcMap were used to perform unified projection transformation, clipping, and mosaicking of the multi-temporal land use data and population spatial distribution data for the HZM-GBAUC, establishing a consistent spatial reference datum. ArcToolbox's spatial statistics tools and raster calculator were employed for land use reclassification, geometric area computation, and subsequent extraction of deeper spatial characteristics such as center-of-gravity migration and hot-cold spot patterns. The software provided both a robust computational environment for large-volume geospatial data and, through its powerful symbology functions, an intuitive representation of the spatio-temporal evolution maps of land and population in the study area [41].

2.4 Research methods

To reveal the spatio-temporal characteristics of land use change across the HZM-GBAUC and their spatial correspondence with population dynamics, this study employs a suite of quantitative geographical methods, including the land use transfer matrix, the center-of-gravity migration model, and spatial hot-cold spot analysis [42].

2.4.1 Land use transfer matrix

The land use transfer matrix is derived from the Markov model in systems analysis and serves as a core method for characterising the direction and magnitude of mutual conversions between different land use types over a given period [43]. The model comprehensively and specifically reflects the flows and sources of each land use type between the initial and terminal time points of the study period [44], thereby quantitatively depicting the competitive dynamics between ecological and construction land during the urbanisation process in the HZM-GBAUC. In ArcMap, cross-conversion area between land use raster or vector layers of different years is typically extracted through spatial overlay analysis or the Tabulate Area tool [45]. The calculation formula is as follows:

$$S_{ij} = \begin{bmatrix} S_{11} & S_{12} & \cdots & S_{1n} \\ S_{21} & S_{22} & \cdots & S_{2n} \\ \vdots & \vdots & \ddots & \vdots \\ S_{n1} & S_{n2} & \cdots & S_{nn} \end{bmatrix}$$

In this expression, S denotes land area; n denotes the total number of land use types in the study area; i and j denote the land use types at the beginning and end of the study period, respectively; the diagonal elements S_{ii} represent the area of land categories that remained unchanged during the study period, while the off-diagonal elements S_{ij} $(i \neq j)$ represent the area converted from land type i to land type j Analysing this matrix allows precise tracking of, for instance, the conversion of water bodies to built-up land through land reclamation, or the encroachment of urban expansion onto forest and agricultural land [46][47].

2.4.2 The center-of-gravity migration model

The concept of the center of gravity originated in physics and was subsequently widely introduced into human and physical geography to describe the overall tendency and migration trajectory of a geographic phenomenon in regional spatial distribution [48]. To examine the spatial expansion preferences of urban built-up land and the dynamic evolution of population agglomeration centers across the HZM-GBAUC, this study employs a spatial center-of-gravity migration model. Using the Mean Centre function within the Measuring Geographic Distributions toolset in ArcMap, the geometric centroid coordinates of specific land use types or population distributions are calculated for each year [49]. The calculation formula is as follows:

$$X_t = \frac{\sum_{i=1}^{n}(C_{it} \times x_i)}{\sum_{i=1}^{n} C_{it}}, Y_t = \frac{\sum_{i=1}^{n}(C_{it} \times y_i)}{\sum_{i=1}^{n} C_{it}}$$

In this expression, X_t and Y_t denote respectively the longitude and latitude coordinates of

the center of gravity of a given geographic element (e.g., built-up land or population) in year t; n is the total number of spatial units in the study area [50]; x_i and y_i are the geometric centroid coordinates of the i-th spatial unit; and $C_{it}$is the attribute value (i.e., land patch area or population count) of the i-th spatial unit in year t. By connecting the centroid points for each period to generate a migration trajectory, the macro-directional tendency of regional development can be intuitively assessed [51].

2.4.3 Spatial hot-cold spot analysis

To further identify the significant local spatial agglomeration characteristics of land use change intensity and population increase or decrease, this study employs the Getis-Ord Gi* index for local spatial autocorrelation (hot-cold spot) analysis [52]. This method overcomes the limitation of global spatial autocorrelation in being unable to specify the exact locations of agglomeration, and effectively detects the specific spatial distribution of high-value clusters (hot spots) and low-value clusters (cold spots) [53]. Using the Hot Spot Analysis tool in ArcMap, the statistic is computed for gridded land change rates or population density increments as follows:

$$G_i^*(d) = \frac{\sum_{j=1}^{n} W_{ij}(d)X_j - \bar{X}\sum_{j=1}^{n} W_{ij}(d)}{S\sqrt{\frac{n\sum_{j=1}^{n} W_{ij}^2(d) - \left(\sum_{j=1}^{n} W_{ij}(d)\right)^2}{n-1}}}$$

In this expression, X_j is the observed value of spatial unit j (e.g., population growth); $W_{ij}(d)$ is the spatial weight matrix based on distance d, taking a value of 1 when spatial units i and j are adjacent and 0 otherwise; $\bar{X}$ is the mean of all observed values; S is the standard deviation of observed values; and n is the total number of spatial units. The resulting G_i^* statistic is the Z-score: when the Z-value is significantly and substantially positive, the area constitutes a 'hot spot' of significant high-value agglomeration (e.g., areas of rapid population growth or intensive land development); conversely, when the Z-value is significantly and substantially negative, the area is a 'cold spot' of low-value agglomeration [53][55]. This analysis assists in revealing the boundaries of spatial heterogeneity in the land–population interaction within the HZM-GBAUC.

3. Results

3.1 Land use types and areas in Hong Kong, Zhuhai, and Macao from 2016 to 2025

Using 2016, 2019, 2022, and 2025 as four temporal benchmarks, and drawing on land use transfer matrices and population centroid data, this study systematically analyses the driving mechanisms of land use change in the region and their implications for population dynamics.

The total study area covers approximately 3,300 km². This study primarily discusses seven major land use categories: built-up land, cropland, forest, grassland, shrubland, water body, and wetland.

Land type	2016	2019	2022	2025	Net change (2016→2025)
Built-up Land	569.00	556.00	537.39	748.28	+179.28
Cropland	656.57	697.66	724.11	290.79	-365.78
Forest	809.96	791.45	787.95	1027.87	+217.91
Grassland	4.11	0.21	0.12	91.97	+87.86
Shrubland	188.57	191.36	194.59	21.81	-166.76
Water	857.32	831.39	832.31	1105.09	+247.77

Wetland	215.45	232.89	224.48	5.01	-210.44

Table 1 Summary of Land Use Areas at Each Temporal Benchmark (km²)

Based on monitoring and analysis of land use data for the HZM-GBAUC from 2016 to 2025, land use types in the study area have evolved from relative stasis to structural transformation. Total area remains stable at between 5,316.97 and 5,325.81 km², with overall growth attributable primarily to human activities such as coastal land reclamation.

The area data for each land use type are shown in Table 1.The data indicate that between 2016 and 2022, built-up land declined marginally from 569.00 km² to 537.39 km². By 2025, built-up land exhibited explosive growth, surging to 748.28 km². Between 2016 and 2022, cropland experienced mild fluctuation and growth, rising from 656.57 km² to 724.11 km². By 2025, cropland fell sharply to 290.79 km², a decline of more than 60%. Forest expanded markedly to 1,027.87 km² in 2025, while grassland area leapt from near-zero to 91.97 km², compensating through afforestation and green restoration for ecological losses caused by built-up expansion. Water body area increased substantially in 2025, rising from 832.31 km² in 2022 to 1,115.09 km². Conversely, both wetland and shrubland contracted to historic lows in 2025, at 5.01 km² and 21.81 km² respectively. The land use type maps of Hong Kong, Zhuhai, and Macau are shown in Figure 2

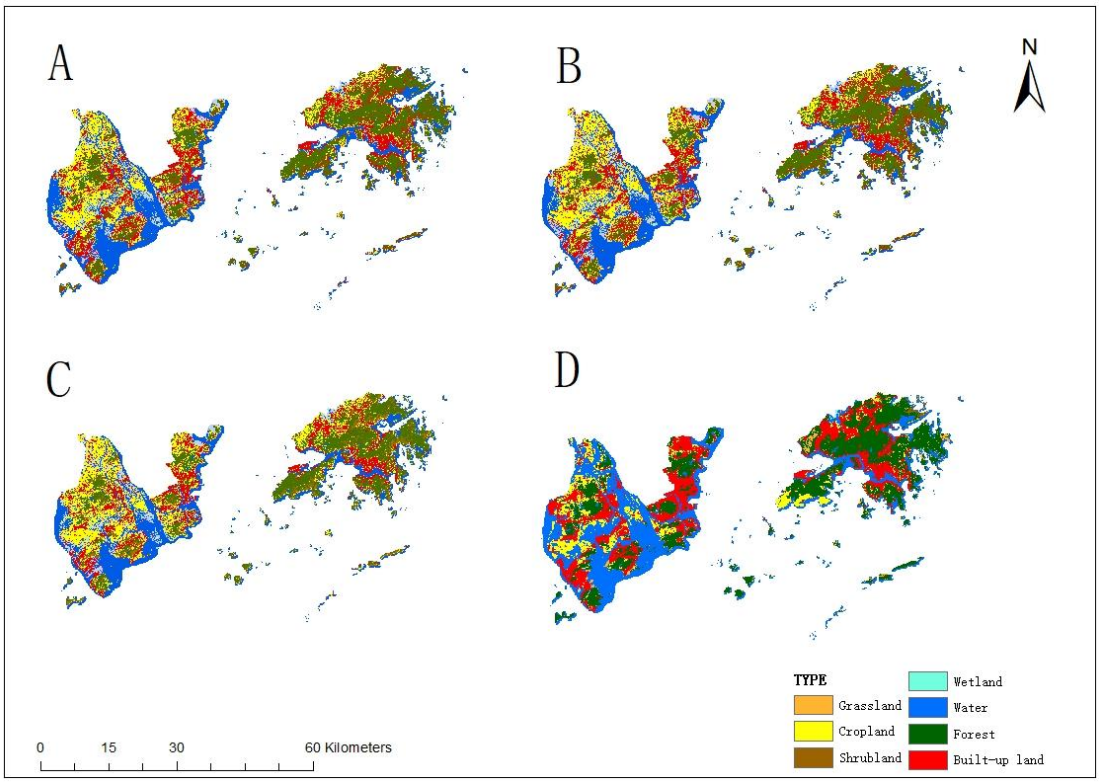


Figure 2 Map of land use types in Hong Kong, Zhuhai, and Macao among different years (A: 2016; B: 2019; C: 2022; D: 2025)

3.2 2016-2025 Land use transfer across Hong Kong, Zhuhai, and Macao

3.2.1 2016-2019

The land use transfer matrix data for 2016-2019 is shown in Table S1. During this phase, built-up land declined slightly from 569.00 km² to 556.00 km², a reduction of approximately 13 km², indicating localised land reversion and ecological restoration activity. Cropland area increased from 656.57 km² to 697.66 km², a net gain of approximately 41 km², while wetland also grew from 215.45 km² to 232.89 km².

The transfer matrix for this phase reveals that built-up land was converted to cropland at 45.83 km² and to wetland at 6.67 km², indicating that in cities such as Zhuhai, portions of development zone land were reclaimed under policy influence. Cropland conversion to built-up land was only 35.17 km² demonstrating phased success for farmland protection policies. The land use transfer map for 2016-2019 is shown in Figure 3, and the Sankey diagram of land use type transfer is shown in Figure 4.

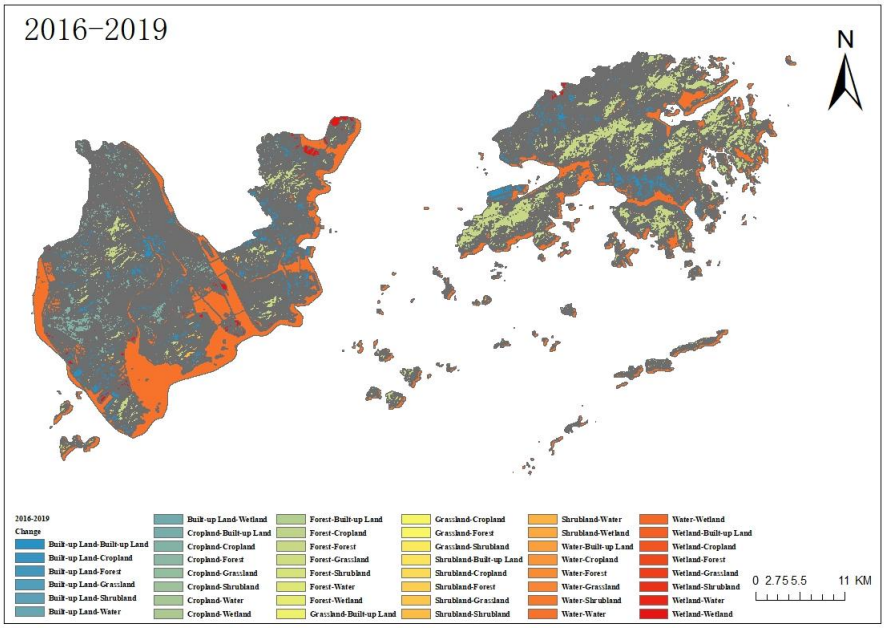


Figure 3 Land use type transfer map from 2016 to 2019

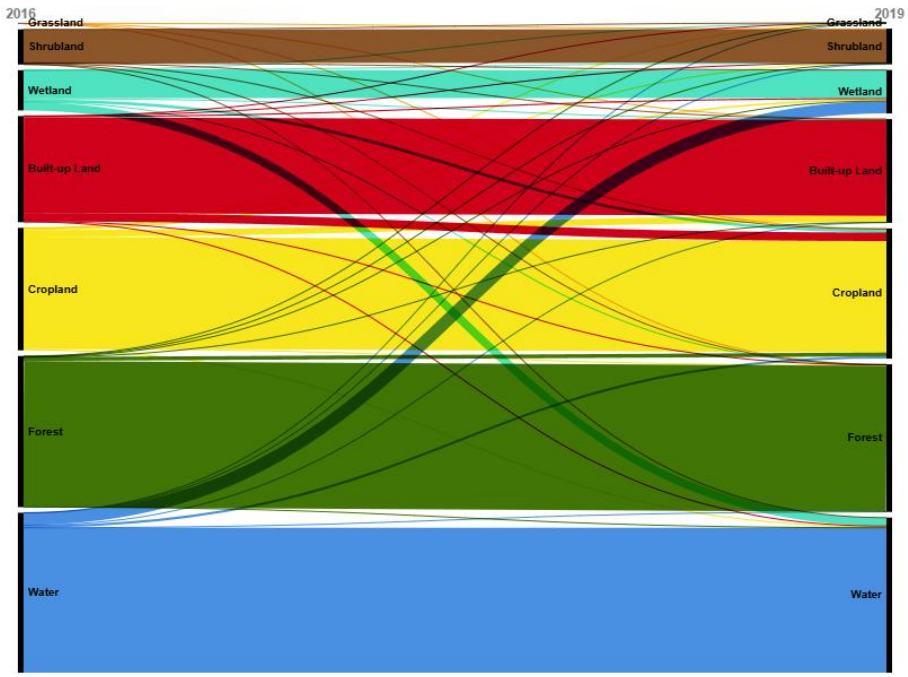


Figure 4 Land use type transfer Sankey map from 2016 to 2019

3.2.2 2019-2022

The land use transfer matrix data for 2019-2022 is shown in Table S2.The magnitude of change in total land categories narrowed further in this phase, with the overall pattern approaching stability.

Built-up land fell to 537.39 km², a combined reduction of approximately 18.6 km² across the three years; cropland steadily increased to 724.11 km², a cumulative gain of 10.2% relative to the 2016 baseline.

Water body area increased marginally from 831.39 km² to 832.31 km², while wetland declined slightly to 224.48 km², reflecting dynamic water–wetland system interconversions: the Hong Kong–Zhuhai–Macao Bridge and associated reclamation works had been substantially completed around 2018, causing surrounding marine ecological disturbance to gradually stabilise as natural wetlands began recovering.

Built-up land contributed 50.25 km² to cropland and 7.43 km² to wetland conversions; cropland contributed 35.72 km² to built-up land, indicating that urban sprawl continued but was effectively offset by policy controls. The land use transfer map for 2019-2022 is shown in Figure 5, and the Sankey diagram of land use type transfer is shown in Figure 6.

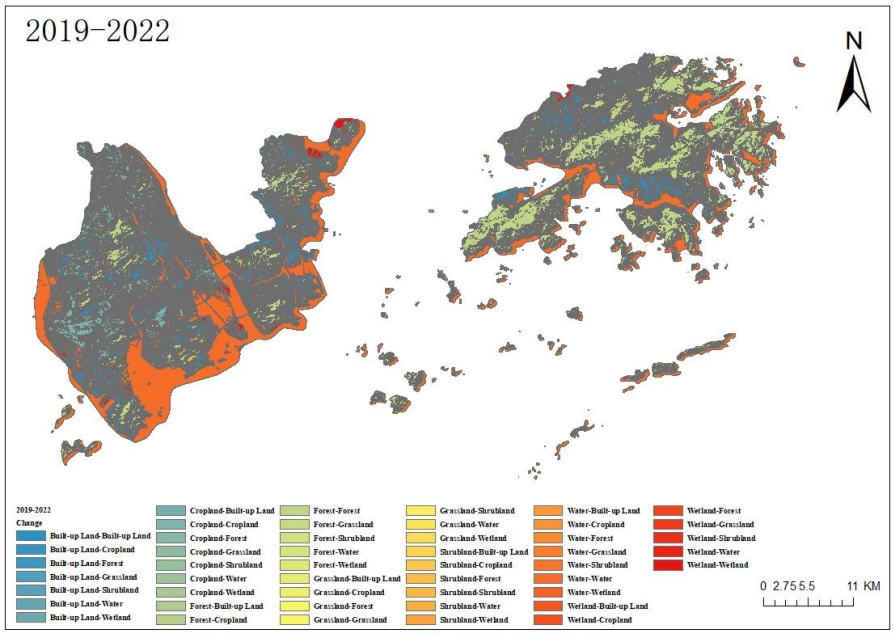


Figure 5 Land use type transfer map from 2019 to 2022

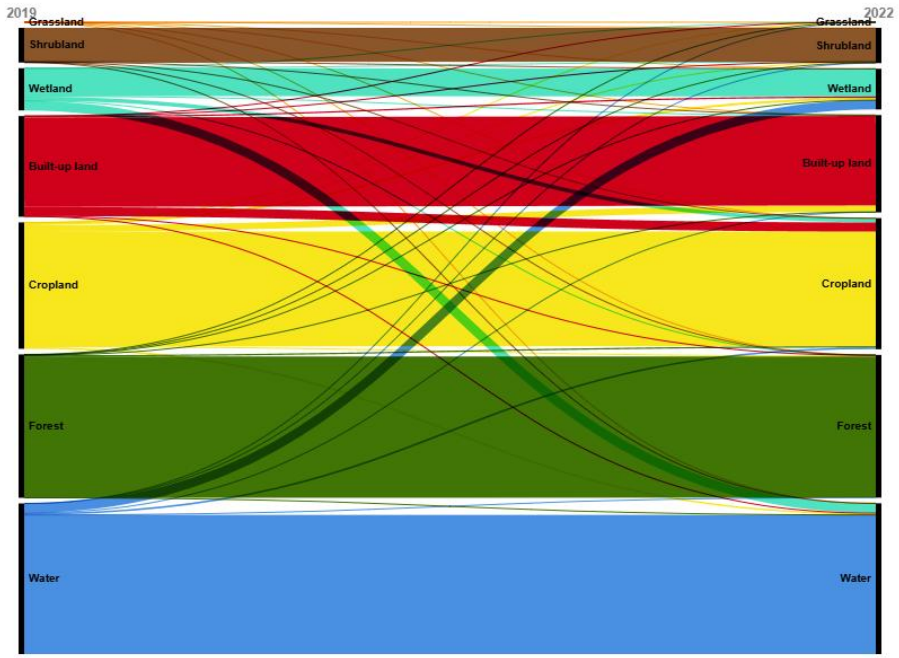


Figure 6 Land use type transfer Sankey map from 2019 to 2022

3.2.3 2022-2025

The land use transfer matrix data for 2022-2025 is shown in

Table S3.This phase witnessed the most intense changes within the study period, with multiple land categories undergoing large-scale restructuring. The most prominent feature is the dramatic shrinkage of cropland (from 724.11 to 290.78 km², a reduction of approximately 433.3 km²), near-disappearance of shrubland (from 194.59 to 21.81 km²), sharp decline of wetland to 5.00 km², substantial expansion of forest (from 787.95 to 1,027.86 km², an increase of approximately 239.91 km²), growth of grassland from near-zero to 91.97 km², increase of water body to 1,107.73 km², and recovery of built-up land to 748.27 km².

Large areas of cropland and shrubland were converted to forest and grassland through ecological restoration projects; portions of reclaimed areas were formally classified as water bodies; multiple major construction projects in Zhuhai, Hong Kong's Northern Metropolis, and elsewhere entered peak land-use phases, driving a net increase of approximately 210 km² in built-up land. The transfer matrix indicates combined outflows from cropland to forest, water body, and built-up land of approximately 490.4 km², and from shrubland to forest of 163.9 km², all are the largest single-phase transfers. The land use transfer map for 2022-2025 is shown in Figure 7, and the Sankey diagram of land use type transfer is shown in Figure 8.

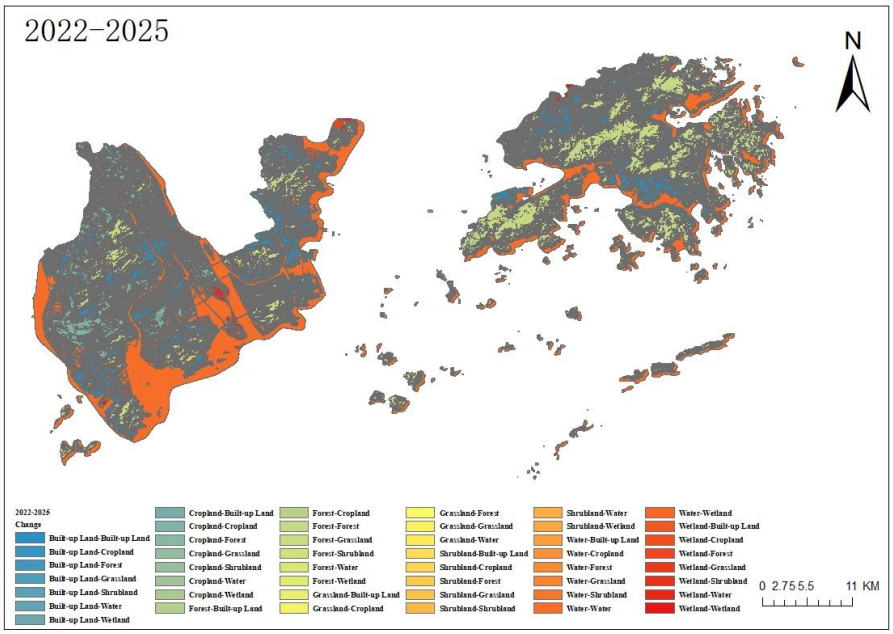


Figure 7 Land use type transfer map from 2022 to 2025

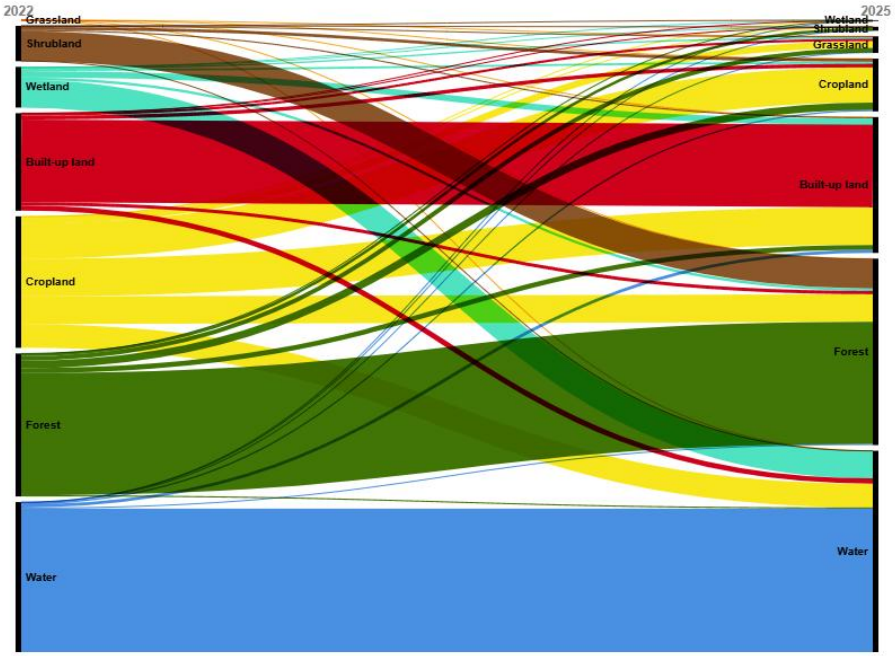


Figure 8 Land use type transfer Sankey map from 2012 to 2025

3.3 Population changes in Hong Kong, Zhuhai, and Macao from 2016 to 2024

Based on analysis of population statistics for 2016, 2019, 2022, and 2024, the HZM-GBAUC has experienced significant population expansion and internal spatial restructuring over the past two decades, each following distinctly different evolutionary logics. The population density distribution map of Hong Kong, Zhuhai, and Macao in 2016-2024 is shown in Figure 9.

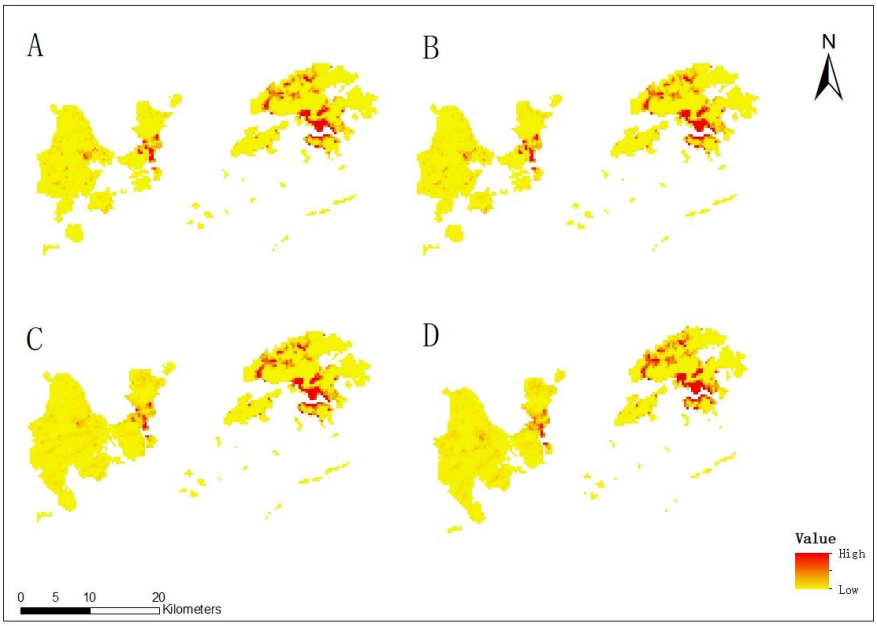


Figure 9 Population density distribution map of Hong Kong, Zhuhai, and Macao (A: 2016; B: 2019; C: 2022; D: 2024)

Population density in Hong Kong's core urban areas showed marked differentiation during the study period (See Table 2). Yau Tsim Mong District recorded the highest density in the territory, approximately 55,309 persons pre km² in 2016, rising to 57,613 persons pre km² in 2022 and remaining extremely high at 58,270 persons pre km² in 2024. Wan Chai District declined continuously from 34,547 persons/km² in 2016 to 29,753 persons pre km² in 2024, a decrease of 13.9%. The Southern District on Hong Kong Island fell from 5,346 to 4,739 persons pre km² (−11.4%), consistent with trends of commercialisation pressure inflating residential costs and residents relocating outward. Tai Po District density rose from 825 to 1,156 persons pre km² (+40.1%), recording the largest increase in the territory; Sai Kung District rose by 23.6%, Yuen Long District by 18.2%, and Tuen Mun District by 13.9%. The North District though at a low base density, also registered positive growth (+4.7%). Kwun Tong District's 2024 population density rose to 26,309 persons pre km², a 17.4% increase from 2016, the most pronounced rise in Kowloon City District. In contrast, the peri-urban Tsuen Wan District and Kwai Tsing Districts fell sharply by 33.2% and 19.5% respectively.

Administrative district	2016	2019	2022	2024	Net change
Central and Western District	14069	14201	13190	15721	▲+11.7%
Wanchai District	34547	34872	32389	29753	▼ -13.9%
Eastern District	6517	6307	5942	6298	▼ -3.4%
Southern District	5346	5397	5011	4739	▼ -11.4%
Yau Tsim Mong District	55309	55812	57613	58270	▲ +5.4%
Sham Shui Po District	39606	39972	411147	39331	▼ -0.7%
Kowloon City District	54567	55064	56841	53795	▼ -1.4%
Wong Tai Sin District	23239	23450	24206	22870	▼ -1.6%
Kwun Tong District	22403	22607	23337	26309	▲+17.4%
Tsuen Wan District	6171	6216	6275	4126	▼ -33.2%
Tuen Mun District	3154	3179	3262	3590	▲+13.9%

Yuen Long District	4992	5018	5007	5898	▲+18.2%
North District	2435	2453	2467	2549	▲ +4.7%
Tai Po District	825	844	845	1156	▲ 40.1%
Sai Kung District	1214	1222	1231	1500	▲ 23.6%
Sha Tin District	5828	5878	5932	5708	▼ -2.1%
Kwai Tsing District	19029	19180	19357	15317	▼ -19.5%
Islands District	660	559	701	695	▲ +5.3%

Note: Population density unit is persons pre km². ▲ denotes increase; ▼ denotes decrease. Net change represents the relative rate of change from 2016 to 2024.

Table 2 Population density data of Hong Kong from 2016 to 2024

Population density data for Macau are shown in Table 3, St. Anthony Parish recorded a population density of 123,636 persons/km² in 2016, the highest in the territory, which plummeted to 67,000 persons pre km² in 2022 before recovering marginally to 68,273 persons pre km² in 2024, representing an overall decline of 44.8%. St. Lawrence Parish density decreased slightly by 2.6%, remaining broadly stable. St. Francis Parish is Macao's most dynamic emerging district in terms of population density growth, rising from 4,450 persons pre km² in 2016 to 6,656 persons pre km² in 2024, an increase of 49.6%. St. Lazarus Parish density surged from 55,167 persons pre km² in 2016 to 87,000 persons/km² in 2024, a remarkable increase of 57.7%. Our Lady of Fatima Parish grew by 18.3% and Cathedral Parish by 29.1%, both maintaining positive growth as principal areas on the Macao Peninsula.

Parish	2016	2019	2022	2024	Net change
Our Lady of Fatima Parish	76,250	81,688	88,688	90,219	▲+18.3%
St. Anthony Parish	123,636	125,000	67,000	68,273	▼ -44.8%
St. Lazarus Parish	55,167	55,167	86,667	87,000	▲ +57.7%
Cathedral Parish	14,471	15,294	18,029	18,676	▲ +29.1%
St. Lawrence Parish	53,700	54,500	50,700	52,300	▼ -2.6%
Our Lady of Carmel Parish	13,316	1,3797	14,316	14,671	▲ +10.2%
St. Francis Parish	4,450	5,033	6,262	6,656	▲ +49.6%

Note: Population density unit is persons pre km². ▲ denotes increase; ▼ denotes decrease. Net change represents the relative rate of change from 2016 to 2024.

Table 3 Population density data of Macao from 2016 to 2024

Population density data for Zhuhai are shown in Table 4. Xiangzhou District, as the urban core of Zhuhai, recorded a population density of 1,736 persons pre km² in 2016, declining to 1,530 persons pre km² in 2022 and remaining broadly flat at 1,536 persons pre km² in 2024. Doumen District population density fell from 730 to 574 persons pre km², a decline of 21.4%, the sharpest decrease among Zhuhai's three districts. Jinwan District density rose from 383 to 433 persons pre km² (+13.1%), briefly peaking at 578 persons pre km² in 2019.

Administrative district	2016	2019	202	2024	Net change
Xiangzhou District	1,736	1,765	1,530	1,536	▼ -11.5%
Doumen District	730	632	577	574	▼-21.4%
Jinwan District	383	578	427	433	▲ 13.1%

Note: Population density unit is persons pre km². ▲ denotes increase; ▼ denotes decrease. Net change represents the relative rate of change from 2016 to 2024.

Table 4 Population density data of Zhuhai City from 2016 to 2024

3.4 Spatial distribution pattern of building land in Hong Kong, Zhuhai, and Macao

The standard deviational ellipses and center-of-gravity migration maps (see Figure 10) indicate that the spatial distribution of built-up land in the HZM-GBAUC exhibits marked directionality. All three standard deviational ellipses display a clear northeast–southwest orientation, demonstrating that built-up land in this region does not expand uniformly but rather clusters and extends along a specific axis. In terms of ellipse area, the range differences across the three standard deviation levels are considerable; the third standard deviational ellipse (red) covers a significantly larger area than the first (blue) and second (yellow), indicating that the overall distribution of built-up land is relatively dispersed with a small number of edge developments located far from the core, while the core agglomeration zone (within the first standard deviational ellipse) remains highly compact.

The center-of-gravity migration trajectory shows that the centroid of built-up land shifted notably from 2016 (red dot) through 2019 (yellow dot) and 2022 (blue dot) towards the southwest, before partially reverting in a southeasterly direction by 2025 (green dot). This trajectory indicates that built-up land expansion was not uniformly distributed across the study period but shifted in emphasis across phases: during the earlier phase (2016-2022), the construction centroid moved towards the southwest, reflecting the relative intensification of construction activities in the Zhuhai and Macao directions; during the later phase (2022-2025), the centroid partially recovered, possibly associated with a phased resurgence of construction activity in Hong Kong and its environs. The overall magnitude of centroid migration is relatively limited, indicating that the spatial pattern of built-up land in the HZM-GBAUC broadly stable at the macro level, with construction activity concentrated within established urbanised core areas.

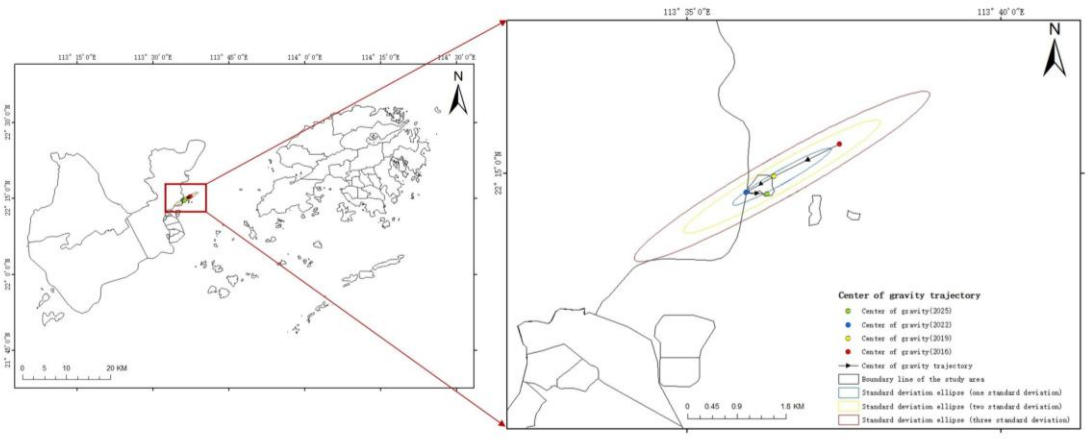


Figure 10 Map of the center of gravity and standard deviation ellipse of the building land in the study area

3.5 Factors that lead to changes in land use

The establishment in 2019 of the HZM-GBAUC's core positioning within the national strategy directly propelled the implementation of large-scale land development plans including Zhuhai's Hengqin New Area and Hong Kong's Northern Metropolis. The rapid recovery of built-up land after 2022 closely coincides with the commencement of substantive development phases for these strategic projects. The sustained decline in built-up land and continuous growth of cropland between 2016 and 2022, contrary to the conventional pattern of net cropland loss driven by urbanization, reflects the strong enforcement of cropland balance policies and the designation of permanent basic

farmland. During this phase, Zhuhai reclaimed portions of urban fringe construction land for cultivation while maintaining a dynamic balance in the compensation for cropland newly occupied by construction. Between 2022 and 2025, forest land across the HZM-GBAUC registered a net increase of approximately 240 km² and grassland of approximately 91 km², closely correlated with the concurrent implementation of ecological corridor restoration in Zhuhai and forest zone expansion in Hong Kong. The large-scale conversion of shrubland to forest is the result of afforestation programmes, reflecting a policy orientation of replacing shrubland with forest to enhance ecosystem quality. Water body area, beyond the effects of reclamation activities, was also influenced by the increased frequency of extreme precipitation events. Growth from 857 km² in 2016 to 1,115 km² in 2025, an increase of approximately 30%, reflects the fact that the HZM-GBAUC has experienced frequent super typhoons and prolonged rainstorms in recent years, causing the extent of seasonal water bodies to be captured in remote sensing imagery statistics. Concurrently, the abrupt decline of wetland to 5.01 km² reflects adjustments in the land classification system: coastal tidal flat areas previously classified as wetland, due to sea-level rise and land reclamation activities, have partially converted to permanent water bodies.

The Hong Kong–Zhuhai–Macao Bridge and associated infrastructure consumed large areas of construction land and water bodies during 2016-2019, and generated substantial reclamation activity, causing localised fluctuations in wetland and water body statistics during that phase. Between 2019 and 2022, project completion and ecological restoration proceeded concurrently, stabilising water body and wetland areas. The Zhuhai Jinwan Airport expansion and auxiliary works for the Shenzhen–Zhongshan Link also accelerated during 2022-2025, directly correlating with the recovery of built-up land.

Based on population centroid migration data, the population center of gravity in the HZM-GBAUC shifted overall in a southwesterly direction during the study period, reflecting the sustained enhancement of population attractiveness on the mainland side of the Greater Bay Area. Population growth driving demand for residential, commercial, and infrastructure uses propelled the significant expansion of built-up land after 2022; while the deceleration or net outflow of Hong Kong's population growth partially relieved land expansion pressure in Hong Kong, contributing to the characteristic pattern of built-up land statistics at the regional level showing a decline-then-rise trajectory. Macao, with its extremely small area and near-saturated land development, has limited influence on regional aggregate change, though its high-density built environment imposes long-term pressure on local ecosystems, primarily manifested in the continued decline of wetlands.

3.6 Analysis of the impact of land use change

The net increase of approximately 210 km² in built-up land from 2022 to 2025 was spatially concentrated in areas such as Hengqin in Zhuhai, the Northern Metropolis development area in Hong Kong, and the Zhuhai Aeronautics and Astronautics Industry Park. This spatial expansion provided critical spatial carriers for emerging industries including biomedicine, integrated circuits, aviation manufacturing, and fintech. The net reduction of approximately 433 km² in cropland from 2022 to 2025 has severely compressed Zhuhai's agricultural production space. Although some losses have been partially offset by urban agriculture and vertical farming within built-up areas, traditional grain and vegetable production functions have been substantively impacted, further reducing regional food self-sufficiency and intensifying dependence on external supply chains. The significant expansion of forest and grassland has enhanced the regional stock of green ecological assets and provided resource foundations for ecological tourism and forest wellness.

The HZM-GBAUC constitutes an important migratory bird corridor globally and provides overwintering habitats for multiple rare and endangered species. The precipitous contraction of wetland area, at a rate of 97.8%, will lead to severe biodiversity decline and habitat fragmentation for migratory birds; reduced coastal protection functions and elevated risk of typhoon-driven storm surges; and diminished offshore water purification capacity with increased probability of harmful algal blooms and eutrophication. The net increase of 218 km² in forest has effectively enhanced regional carbon sequestration capacity, water conservation functions, and biodiversity corridor connectivity, making a positive contribution to offsetting the carbon emission increment generated by built-up land expansion. However, the concurrent significant increase in built-up land intensifies urban heat island effects, simultaneously creating pressure on the region's carbon reduction targets. The expansion of water body area, on the one hand, enhances regional flood regulation capacity and enriches waterfront landscape resources; on the other hand, the extensive expansion of permanent water bodies alters local hydrodynamic conditions, with certain impacts on fish spawning habitats and the distribution of benthic biological communities.

The study's land use typology encompasses seven categories: built-up land, cropland, forest, grassland, shrubland, water and wetland. Among these, built-up land exhibits the most pronounced change during the study period; the following analysis therefore focuses primarily on the impact of built-up land change on population dynamics. According to the land use analysis data, built-up land in the HZM-GBAUC underwent a phased trajectory of initial decline followed by recovery between 2016 and 2024: from 2016 to 2022, built-up land contracted modestly from 569 km² to 537 km², then surged sharply from 2022 to 2025 to 748 km², a net increase of approximately 210 km². From the population density distribution maps, high-density agglomeration zones (darker areas) are increasingly concentrated in the Kowloon–Hong Kong Island corridor, while low-density dispersal zones extend towards the southwest, corroborating the northeast-to-southwest migration trajectory of the built-up land centroid.

Population density data indicate that density growth in the northern districts (Tai Po District, Sai Kung District and Yuen Long District) aligns closely with land development in this direction, while the declining density in older districts such as Wan Chai District, Tsuen Wan District, and Kwai Tsing District reflects the initial manifestation of population deconcentration effects. In Macao, the incremental built-up land is primarily derived from continued development of St. Francis Parish reclamation area, which not only provides new residential and commercial space but has also become the fastest-growing area in terms of population density. The establishment of the Hengqin Guangdong–Macao In-Depth Cooperation Zone has further extended Macao's population carrying hinterland, objectively relieving population pressure in the Macao Peninsula, enabling older areas such as St. Anthony Parish to achieve some decompression despite extremely high population densities.

The opening of the Hong Kong-Zhuhai-Macao Bridge in 2018 broke the physical isolation among the HZM-GBAUC. The rapid expansion of built-up land in areas adjacent to the bridge's landing points in Zhuhai stimulated population growth in Jinwan District; the construction of reclaimed new zones and port facilities on the Macao side also accelerated population agglomeration in St. Francis Parish area; and Hong Kong's Lantau Islands District, as the bridge's Hong Kong terminal, has seen its land development gradually intensify, with population density increasing from 660 to 695 persons pre km², laying the foundation for subsequent Northern Metropolis development.

4. Discussion

4.1 Policy-Guided Spatial Interactions among Land Use, Population, and Ecology

This study reveals the dominant mechanism of policy intervention in reshaping land-population feedback relationships. Land use change and its spatial configuration across the HZM-GBAUC between 2016 and 2025 represent the core factors shaping population redistribution in this high-density cross-boundary urban agglomeration. The implementation of the Outline Development Plan for the Guangdong-Hong Kong-Macao Greater Bay Area in 2019 shifted the regional governance paradigm from administrative isolation to cross-boundary functional integration. This policy mandated the convergence of infrastructure and relaxed institutional barriers for cross-border businesses, which directly catalyzed large-scale infrastructure investment [57]. Particularly between 2022 and 2025, Zhuhai's policy designation as a key West-Bank node with relaxed talent-entry thresholds and subsidized industrial land quotas created a policy pull effect. This institutional incentive converted built-up land expansion directly into a structured population vacuum, drawing over 2.5 million permanent residents [58]. The built-up land expansion and population growth exhibit a clearly positive correlation. In 2021, Hong Kong's Northern Urban Development Strategy initiated a structural shift in land supply, aiming to direct residential and industrial development northward, closer to the periphery. Hong Kong's built-up land development strategy is oriented primarily towards northern New Territories areas such as Tai Po District, Yuen Long District and the North District; through large-scale residential land supply, it guides residents from high-density Kowloon and Hong Kong Island to relocate outward [59]. This was not merely a passive land supply shift, but a deliberate policy-driven de-concentration strategy designed to alleviate the socio-spatial pressure of the southern core and leverage the economic spillover of the mainland-border economy, thereby directing the population gravity southwestward.

Throughout the study period, the spatial competition between built-up land and ecological land was intense. Afforestation and green restoration projects drove net increases in forest and notable growth in grassland, partially enhancing regional carbon sink capacity and ecological connectivity [60]. The simultaneous sharp decline of wetland area represents a land cover conversion that not only exacerbates habitat fragmentation for migratory birds and increases the risk of typhoon storm surges, but also imposes long-term spatial environmental stress on coastal biodiversity and vulnerable populations. Zhuhai, drawing on the ecological endowment of the Wanshan Islands and Hengqin wetlands, has already formed an embryonic coastal ecotourism product portfolio; the expansion of Hong Kong's country parks similarly strengthens its global green city profile, attracting high-end tourism and convention-economy activity.

4.2 Institutional Intervention Strategies for Global Cross-Boundary Urban Agglomerations

The HZM-GBAUC, as one of the most institutionally diverse cross-boundary urban agglomerations in the world, faces a land–population trade-off challenge that is not unique but rather a typical bottleneck encountered by mega-scale trans-boundary urban regions globally during deep integration processes [61]. High institutional and economic gradients, mediated through differences in land policy, can readily lead to regional spatial resource misallocation and destructive competition.

The Singapore–Johor model employs a core–hinterland collaborative development approach. Given the extreme scarcity of land in Hong Kong and Macao contrasted with the spatial potential of Zhuhai's hinterland, it is recommended to establish a land quota coordination mechanism that

transcends administrative and customs boundaries [62]. In population and industry mobility planning, moving beyond a unidirectional land development model and coordinating the stock renewal of high-density core areas with the incremental development of hinterland cities would be advisable. Through the construction of cross-boundary joint parks, the orderly movement of population, especially high-caliber talent, towards newly developed areas could be facilitated, substantively alleviating spatial saturation and social compression effects in older districts. The substantial contraction of wetland in the HZM-GBAUC and degradation of coastal habitats has reached a scale where localised administrative intervention can no longer halt the overall decline of the ecosystem. Drawing on the successful experience of the Oresund region in transnational ecological co-governance and joint maritime spatial planning [63], it is recommended that local governments establish cross-boundary ecological compensation frameworks with genuine binding force and joint environmental monitoring networks. While advancing cross-sea infrastructure and reclamation activities, ecological red-lines and cross-regional wetland restoration plans should be incorporated into the joint statutory planning of the HZM-GBAUC, ensuring that urban expansion does not come at the cost of regional climate resilience. The San Diego-Tijuana metropolitan area on the US-Mexico border has experienced spatial misallocation and tidal cross-border congestion due to institutional disparities and income differentials [64]; the HZM-GBAUC, when leveraging land expansion to guide cross-boundary population redistribution, should go beyond providing mere physical housing supply. Governments should strive to advance equitable cross-boundary public service reforms. The research findings indicate that only when the supply of social public services in new expansion areas can smoothly interface with, or even match, core area standards will policy-led population transfer across administrative boundaries successfully transform into voluntary integration driven by the pursuit of a higher quality of life.

In sum, this study has, within a unified conceptual framework, comprehensively assessed the spatio-temporal transformation of land use across the HZM-GBAUC and the mechanisms through which it influences population dynamics. The directed expansion of built-up land and the coordinated migration of the population center of gravity demonstrate that systematic land planning that transcends the traditional supply-and-demand framework is fundamental to achieving balanced population distribution in high-density urban agglomerations. As regional integration continues to deepen [64], incorporating diversified residential land supply, cross-boundary population mobility guidance, and rigorous coastal ecosystem protection into a comprehensive decision-making framework is essential both for safeguarding regional ecological security and for advancing the sustainable development of high-density cross-boundary urban agglomerations globally.

5. Limitations

The land use data employed in this study span multiple sources, including the GLC_FCS30D global 30-metre resolution land cover dynamic product and the 2025 data released by the National Geomatics Centre of China. Cloud cover interference in remote sensing imagery and seasonal variations in surface conditions may affect the extraction accuracy of water bodies and wetlands in certain periods.

Furthermore, the spatial statistical units for population data in this study vary in granularity, making rigorous grid-based comparison within a unified spatial analysis framework difficult, a limitation that constrains the comparability and precision of hot-cold spot analysis across cities to some degree. Given the close spillover and linkage effects between population flows and land

development in the HZM-GBAUC and surrounding cities, research conclusions focusing only on these three locations have limited extrapolation capacity to the broader and more complex Bay Areas. Future research could reconstruct analytical units at a larger spatial scale that transcends administrative boundaries.

6. Conclusion

The land use pattern of the HZM-GBAUC underwent an evolution from relative stasis to structural transformation during the study period. Between 2016 and 2022, constrained by policy and stock-planning orientations, the total volume of built-up land exhibited a gentle contracting trend, cropland area steadily recovered, and land-intensification management policies achieved phased outcomes. Between 2022 and 2025, as the Guangdong-Hong Kong-Macao Greater Bay Area strategy advanced in depth, built-up land registered a net increase of approximately 210 km², while forest and grassland expanded markedly in the same period, forming a composite pattern in which development and ecological restoration advanced in parallel, yet the precipitous decline of wetland to historic lows reveals the severe pressure confronting coastal ecosystem protection. Population space in the HZM-GBAUC displays pronounced differentiation: Zhuhai progressively achieved region-wide population agglomeration anchored to the Greater Bay Area strategy; Hong Kong's population space continued to consolidate from the core towards peripheral new development zones in the northern New Territories, closely aligned with the trajectory of built-up land expansion; Macao's population distribution, facilitated by large-scale land development in St. Francis Parish reclamation area, has undergone directed transfer towards newly completed built zones. The direction, scale, and pace of built-up land expansion are positively correlated in space with the hot-cold patterns of population density across the cities, corroborating the fundamental principle that land development activity serves as the core driver of population agglomeration.

Declarations

Ethics approval and consent to participate

Not applicable.

Consent for publication

Not applicable.

Availability of data and materials

The author confirms that all data generated or analyzed during this study are included in this published article. Furthermore, primary and secondary sources and data supporting the findings of this study were all publicly available at the time of submission.

Competing interests

The authors declare no competing interests.

Funding

This research was not funded.

7.References

[1] Long, H., Zhang, Y., Ma, L., & Tu, S. (2021). Land use transitions: Progress, challenges and prospects. *Land*, *10*(9), 903.

[2] Scheidel, A., & Sorman, A. H. (2012). Energy transitions and the global land rush: Ultimate drivers and persistent consequences. *Global environmental change*, *22*(3), 588-595.

[3] Marshall, J. D. (2007). Urban land area and population growth: A new scaling relationship for metropolitan expansion. *Urban studies*, *44*(10), 1889-1904.
[4] Qu, Y., & Long, H. (2018). The economic and environmental effects of land use transitions under rapid urbanization and the implications for land use management. *Habitat International*, *82*, 113-121.
[5] Chu, X., & Xu, L. (2025). The research progress and future frontiers of agricultural geography: A comprehensive review of theoretical evolution, technological transformation, and practice-driven development. *Geographical Research Bulletin*, *4*, 680-723.
[6] Singh, N., Singh, S., & Mall, R. K. (2020). Urban ecology and human health: implications of urban heat island, air pollution and climate change nexus. In *Urban ecology* (pp. 317-334). Elsevier.
[7] Yue, X., Wang, Y., Li, W., Wu, Y., Wang, Y., Zhang, H. O., & Ma, Z. (2024). Research progress and trends in urban residential segregation. *Buildings*, *14*(7), 1962.
[8] Lambin, E. F., & Geist, H. J. (Eds.). (2008). *Land-use and land-cover change: local processes and global impacts*. Springer Science & Business Media.
[9] Rimal, B., Zhang, L., Keshtkar, H., Haack, B. N., Rijal, S., & Zhang, P. (2018). Land use/land cover dynamics and modeling of urban land expansion by the integration of cellular automata and markov chain. *ISPRS International Journal of Geo-Information*, *7*(4), 154.
[10] Li, Y., Ma, X., Zhao, J., Zhang, S., & Liu, C. (2025). Spatio-Temporal Evolution and Conflict Diagnosis of Territorial Space in Mountainous–Flatland Areas from a Multi-Scale Perspective: A Case Study of the Central Yunnan Urban Agglomeration. *Land*, *14*(4), 703.
[11] Scanlon, B. (2024). The geopolitics of infrastructure and the unmaking of an island: The Hong Kong-Zhuhai-Macau Bridge. *Geopolitics*, *29*(2), 444-470.
[12] Chhabra, A., Geist, H., Houghton, R. A., Haberl, H., Braimoh, A. K., Vlek, P. L., ... & Lambin, E. F. (2006). Multiple impacts of land-use/cover change. In *Land-use and land-cover change: local processes and global impacts* (pp. 71-116). Berlin, Heidelberg: Springer Berlin Heidelberg..
[13] Basu, D. N., & Kashyap, S. P. (1996). way. Instead of hierarchical mapping of priorities and programmes, ACRP begins with space specific resources (land, water, climatic features). *Agro-climatic Regional Planning in India: Themes and case studies*, *2*, 27.
[14] Zuo, Y., Yang, C., Xin, G., Wu, Y., & Chen, R. (2023). Driving mechanism of comprehensive land consolidation on urban–rural development elements integration. *Land*, *12*(11), 2037.
[15] Li, Z., Lin, K., & Tian, H. (2019). The development of a conservation-oriented and environmentally friendly ecological economy. In *Chinese Dream and Practice in Zhejiang–Ecology* (pp. 29-94). Singapore: Springer Singapore.
[16] So, B. K., Lui, I. D., Wat, K. P., Bai, Y., Lam, K. F., & Yip, P. S. (2025). Assessment of the impact of migration on Hong Kong's population and its development. *Asian Population Studies*, *21*(3), 243-256.
[17] Lam, G., & Tu, E. J. C. (2015). Hong Kong's population policies on immigration: challenges and feasibility. *Asian Education and Development Studies*, *4*(2), 180-189.
[18] Sheng, M., & Gu, C. (2018). Economic growth and development in Macau (1999–2016): The role of the booming gaming industry. *Cities*, *75*, 72-80.
[19] Yang, W. (2024). Strategies for Talent Acquisition and Development: Policies for Enhancing University Talent Growth in the Guangdong-Hong Kong-Macao Greater Bay Area. *Cultura: International Journal of Philosophy of Culture and Axiology*, *21*(5).
[20] Tang, X., Xu, J., Wang, R., Li, J. V., Jiang, L., & Li, C. Z. (2026). Drivers of Cross-Boundary

Land Use and Cover Change in a Megacity Region: Evidence from the Guangdong–Hong Kong–Macao Greater Bay Area. *Sustainability*, *18*(1), 470.
[21] Yu, H. (2024). Regional development in China under the "dual-circulation" strategy: The case of Guangdong-Hong Kong-Macau greater bay area. *Journal of Contemporary China*, *33*(148), 683-703.
[22] Dunford, M., & Perrons, D. (1994). Regional inequality, regimes of accumulation and economic development in contemporary Europe. *Transactions of the Institute of British geographers*, 163-182.
[23] Lam, K. W. K., & Fong, E. (2025). The impact of post-2019 migration on Hong Kong population dynamics. In *Global Hong Kong* (pp. 145-160). Routledge.
[24] Liu, Y., & He, S. (2024). From the Pearl River Delta to the Greater Bay Area: State spatial selectivity, contingent socio-spatial processes, and variegated geographies of China's city-regionalism. *Transactions in Planning and Urban Research*, *3*(3), 216-240.
[25] Weng, M., Qiu, Y., Wu, J., & Li, X. Spatial correlation network characteristics and driving mechanisms of the construction industry in southeastern coastal urban agglomerations of China. *Available at SSRN 5646372*.
[26] Zheng, L., Zheng, Y., & Fu, Z. (2024). The Impact of Urban Renewal on Spatial–Temporal Changes in the Human Settlement Environment in the Yangtze River Delta, China. *Land*, *13*(6), 841.
[27] Zhu, J., Jiang, Y., & Wang, C. (2026). From spatial mismatch to urban equity: a governance-oriented supply–demand coupling framework for evaluating urban park green space equity in high-density Tianjin. *International Journal of Urban Sciences*, 1-36.
[28] Leung, R. C. T. (1978). *Hong Kong, a case of urban settlement expansion: an investigation of implications of waterborne and hillside development* (Doctoral dissertation, Massachusetts Institute of Technology).
[29] Bosselmann, P., & Moos, S. (2014). The metropolitan landscapes of the pearl river delta and the San Francisco Bay Area. *Built Environment*, *40*(2), 244-264.
[30] Löffler, E. (1982). Landforms and landform development. In *Biogeography and Ecology of New Guinea: Part One-Seven* (pp. 57-72). Dordrecht: Springer Netherlands.
[31] Tang, U. W., & Sheng, N. (2009). Macao. *Cities*, *26*(4), 220-231.
[32] Wang, Z., Xu, G., Bao, C., Xu, J., & Sun, F. (2017). Spatial and economic effects of the Bohai Strait Cross-Sea Channel on the transportation accessibility in China. *Applied Geography*, *83*, 86-99.
[33] Shi, Y., Shi, S., & Wang, H. (2019). Reconsideration of the methodology for estimation of land population carrying capacity in Shanghai metropolis. *Science of the Total Environment*, *652*, 367-381.
[34] Mak, H. W. L., & Ng, D. C. Y. (2021). Spatial and socio-classification of traffic pollutant emissions and associated mortality rates in high-density Hong Kong via improved data analytic approaches. *International Journal of Environmental Research and Public Health*, *18*(12), 6532.
[35] Zou, Z., Zhao, X., Liu, S., & Zhou, C. (2025). Driving forces and future scenario simulation of urban agglomeration expansion in China: a case study of the Pearl River Delta urban agglomeration. *Remote Sensing*, *17*(14), 2455.
[36] Zhang, X., Liu, L., Zhao, T., Chen, X., Lin, S., Wang, J., ... & Liu, W. (2023). GWL_FCS30: a global 30 m wetland map with a fine classification system using multi-sourced and time-series remote sensing imagery in 2020. *Earth System Science Data*, *15*(1), 265-293.

[37] Zhang, X., Liu, L., Zhao, T., Gao, Y., Chen, X., & Mi, J. (2022). GISD30: Global 30 m impervious-surface dynamic dataset from 1985 to 2020 using time-series Landsat imagery on the Google Earth Engine platform. *Earth System Science Data*, *14*(4), 1831-1856.
[38] Zhang, X., Liu, L., Chen, X., Gao, Y., Xie, S., & Mi, J. (2021). GLC_FCS30: Global land-cover product with fine classification system at 30 m using time-series Landsat imagery. *Earth System Science Data*, *13*(6), 2753-2776.
[39] Dobson, J. E., Bright, E. A., Coleman, P. R., Durfee, R. C., & Worley, B. A. (2000). LandScan: a global population database for estimating populations at risk. *Photogrammetric engineering and remote sensing*, *66*(7), 849-857.
[40] Liu, T., Luo, Y., Pang, P. C. I., & Xia, Y. (2024). Leveraging digital technologies for public health education in High-Density community spaces: A Geospatial analysis. *Systems*, *12*(11), 504.
[41] Daghlavi, M., Ghasemi-Nejad-Raeini, M., Marzban, A., Taki, M., Moazami, M., & Nabavi-Pelesaraei, A. (2026). High-precision crop rotation mapping in arid agroecosystems: integrating sentinel-2 time series, SVM, and GIS. *Scientific Reports*.
[42] Su, X., Liu, T., Pang, P., Luo, Y. T., & Wong, D. (2026). How Can Large Language Models Drive Environmental Sustainability? A Systematic Scoping Review. *Sustainability*, *18*(9), 4327.
[43] Peng, H., Lou, H., Zhang, Y., Wang, W., He, Q., Liu, P., & Yang, Y. (2025). Study of identification and simulation of ecological zoning through integration of landscape ecological risk and ecosystem health. *Frontiers in Ecology and Evolution*, *13*, 1662739.
[44] Luo, Y. T., Liu, T., Pang, P., & Kan, H. Y. (2026). Decoding dynamic emotional valence in GenAI interactions: insights from covariate-dependent Markov chains. *Frontiers in Psychology*, *17*, 1783364.
[45] Hurtt, G. C., Chini, L. P., Frolking, S., Betts, R. A., Feddema, J., Fischer, G., ... & Wang, Y. P. (2011). Harmonization of land-use scenarios for the period 1500–2100: 600 years of global gridded annual land-use transitions, wood harvest, and resulting secondary lands. *Climatic change*, *109*(1), 117.
[46] Sun, Q., Wu, Z., & Tan, J. (2012). The relationship between land surface temperature and land use/land cover in Guangzhou, China. *Environmental Earth Sciences*, *65*(6), 1687-1694.
[47] Liu, J., Liu, B., Wu, L., Miao, H., Liu, J., Jiang, K., ... & Liu, T. (2024). Prediction of land use for the next 30 years using the PLUS model's multi-scenario simulation in Guizhou Province, China. *Scientific Reports*, *14*(1), 13143.
[48] Alshayeb, M. J. (2025). Evaluating ecosystem service trade-offs and recovery dynamics in response to urban expansion: implications for sustainable management strategies. *Sustainability*, *17*(5), 2194.
[49] Capoani, L. (2023). Review of the gravity model: origins and critical analysis of its theoretical development. *SN Business & Economics*, *3*(5), 95.
[50] Ma, M., Liu, Y., Wang, B., Yan, X., & Li, H. (2023). Spatial-temporal evolution and driving mechanism of urban land use efficiency based on T-DEA model: a case study of anhui province, China. *Sustainability*, *15*(13), 10087.
[51] Muyibul, Z., & Abulizi, M. (2026). Evolutionary characteristics of production, living, and ecological spaces and related environmental effects in Urumqi, Northwest China. *Environment, Development and Sustainability*, *28*(5), 12533-12555.
[52] Zhou, H., Liu, Y., & Liu, Y. (2019). An approach to tracking meteorological drought migration. *Water Resources Research*, *55*(4), 3266-3284.

[53] Songchitruksa, P., & Zeng, X. (2010). Getis–Ord spatial statistics to identify hot spots by using incident management data. *Transportation research record*, *2165*(1), 42-51.
[54] Wang, G., Wang, Y., Li, Y., & Chen, T. (2023). Identification of urban clusters based on multisource data—an example of three major urban agglomerations in China. *Land*, *12*(5), 1058.
[55] Anselin, L. (1992). Spatial data analysis with GIS: an introduction to application in the social sciences.
[56] Yang, M., Ma, J., Jia, P., Pu, Y., & Chen, G. (2011, June). The use of spatial autocorrelation to analyze changes in spatial distribution patterns of population density in Jiangsu province, China. In *2011 19th International Conference on Geoinformatics* (pp. 1-6). IEEE.
[57] Xiao, Y. (2025). *The Guangdong-Hong Kong-Macao Greater Bay Area: The Challenge of Economic and Political Integration* (Doctoral dissertation, University of Liverpool).
[58] Jahid, M. S. R. (2022). Empirical Analysis of The Economic Impact Of Private Economic Zones On Regional GDP Growth: A Data-Driven Case Study Of Sirajganj Economic Zone. *American Journal of Scholarly Research and Innovation*, *1*(02), 01-29.
[59] Wu, Y., Wang, J., & Gou, A. (2023). The evolution characteristics and driving mechanism of urban construction land in Hong Kong since 1972. *Applied Sciences*, *13*(4), 2565.
[60] Huang, T., Ma, L., Wang, X., Sheng, X., Huang, M., & Wang, Y. (2026). Carbon Neutrality Pathways Through Ecological Restoration: Synergies Between Climate Change Mitigation and Degradation Control. *Land Degradation & Development*.
[61] Lee, S., & Lee, S. (2021). *China's water resources management*. Springer International Publishing.
[62] Hutchinson, F. E. (2021). In the gateway's shadow: Interactions between Singapore's Hinterlands. *Growth and Change*, *52*(1), 71-87.
[63] MORF, A., SANDSTEN, J., PRUTZER, M., & LINDROTH, N. (2021). *Blue Economy and Coastal Development–Sharing Swedish Experiences* (No. 2021, p. 5). Report.
[64] Herzog, L. A. (2018). The US–Mexico transfrontier metropolis: Theoretical and empirical explorations. In *Handbook of emerging 21st-century cities* (pp. 222-243). Edward Elgar Publishing.
[65] Wu, L., Lang, W., & Chen, T. (2024). Deciphering Urban Land Use Patterns in the Shenzhen–Dongguan Cross-Boundary Region Based on Multisource Data. *Land*, *13*(2), 161.

Table S1 Land Use Transfer Matrix in Hong Kong, Zhuhai, and Macao from 2016 to 2019(km²):

Summation term: area	2019							
2016	Built-up Land	Cropland	Forest	Grassland	Shrubland	Water	Wetland	Total
Built-up Land	512.7687	45.8298	0.5103	0.0369	0.099	3.0861	6.6735	569.0043
Cropland	35.1684	597.6423	5.1795	0.0855	2.502	6.9462	9.0414	656.5653
Forest	0.7587	20.5713	782.73	0.0018	4.8186	0.297	0.7848	809.9622
Grassland	0.009	0.0756	0.1611	0.0000	3.861	0.0000	0.0000	4.1067
Shrubland	0.3168	5.6979	2.2905	0.0702	180.0405	0.0261	0.1251	188.5671
Water	1.656	12.2355	0.1872	0.0063	0.0135	777.0897	66.1284	857.3166
Wetland	5.3244	15.6069	0.3888	0.0135	0.0297	43.9452	150.1371	215.4456
Total	556.002	697.6593	791.4474	0.2142	191.3643	831.3903	232.8903	3300.9678

Table S2 Land Use Transfer Matrix in Hong Kong, Zhuhai, and Macao from 2019 to 2022(km²):

Summation term: area	2022							
2019	Built-up land	Cropland	Forest	Grassland	Shrubland	Water	Wetland	Total
Built-up land	494.4321	50.2452	0.6588	0.0324	0.2763	2.925	7.4322	556.002
Cropland	35.7192	632.5182	5.7915	0.0342	3.1149	8.2935	12.1878	697.6593
Forest	0.729	7.4529	779.2092	0.0072	3.2742	0.1809	0.594	791.4474
Grassland	0.018	0.1341	0.0009	0.0477	0.0018	0.0009	0.0108	0.2142
Shrubland	0.0999	2.1375	1.2717	0.0000	187.7607	0.0189	0.0756	191.3643
Water	2.1825	9.72	0.2889	0.0009	0.0288	768.1734	50.9958	831.3903
Wetland	4.2093	21.9069	0.7299	0.0009	0.1359	52.722	153.1854	232.8903
Total	537.39	724.1148	787.9509	0.1233	194.5926	832.3146	224.4816	3300.9678

Table S3 Land Use Transfer Matrix in Hong Kong, Zhuhai, and Macao from 2022 to 2025(km²):

Summation term: area	2025							
2022	Built-up land	Cropland	Forest	Grassland	Shrubland	Water	Wetland	Total
Built-up land	454.4278	20.5034	18.3762	13.1771	0.9183	29.0527	0.2613	536.7168
Cropland	207.2589	192.8800	152.1007	37.2413	3.0127	130.6661	0.2166	723.3763
Forest	27.2661	41.5226	671.9100	23.7545	15.1131	6.5993	0.3743	786.5398
Grassland	0.0773	0.0060	0.0176	0.0178	0.0000	0.0046	0.0000	0.1233
Shrubland	6.8498	16.7161	163.9054	4.8538	1.1312	0.7798	0.0792	194.3152
Water	16.7104	7.7219	6.1198	4.1584	0.8317	789.2763	0.5114	825.3298
Wetland	34.9980	11.2254	13.8236	8.4530	0.6132	151.3484	3.5289	223.9906
Total	747.5882	290.5753	1026.2533	91.6558	21.6202	1107.7272	4.9717	3290.3918